*International Journal of Thermophysics, Vol. 23, No. 2, March 2002 (© 2002)*

# Development of a Laser Interferometric Dilatometer for Measurements of Thermal Expansion of Solids in the Temperature Range 300 to 1300 K

**Hiromichi Watanabe,[1, 2] N. Yamada,[1] and M. Okaji[1]**

*Received August 20, 2001*

A laser interferometric dilatometer has been developed for measuring linear thermal expansion coefficients of reference materials for thermal expansion in the temperature range 300 to 1300 K. The dilatometer is based on an optical heterodyne interferometer capable of measuring length change with an uncertainty of 0.6 nm. Linear thermal expansion coefficients of silicon were measured in the temperature range 700 to 1100 K. The performance of the present dilatometer was tested by a comparison between the present data and the data measured with the previous version of the present dilatometer and the data recommended by the Committee on Data for Science and Technology (CODATA). The present data agree well with the recommended values over all the temperature range measured. On the other hand, the present values at lower temperatures are in poor agreement with the previous experimental data. The combined standard uncertainty in the present value at 900 K is estimated to be $1.1 \times 10^{-8}\ \mathrm{K}^{-1}$.

**KEY WORDS:** laser interferometric dilatometer; optical heterodyne interferometer; silicon; thermal expansion coefficient.

## 1. INTRODUCTION

The present study on a laser interferometric dilatometer was triggered by the requirement of the development of reference materials for thermal expansion. Reference materials whose thermal expansion coefficients are accurately determined are essential for calibrating and testing relative measurement devices for thermal expansion such as push-rod dilatometers.

[1] National Metrology Institute of Japan, AIST, AIST Tsukuba Central 3, 1-1-1 Umezono, Tsukuba 305-8563, Japan.

[2] To whom correspondence should be addressed. E-mail: hiromichi-watanabe@aist.go.jp



0195-928X/02/0300-0543/0 © 2002 Plenum Publishing Corporation

However, there has been a lack of both amount and variation of the reference materials for certification in accredited national laboratories. For example, Standard Reference Materials (SRMs) are supplied by the National Institute of Standard and Technology (NIST) in the United States. Since the NIST no longer produces a new stock of SRMs, only the following three kinds of SRMs are presently available:

SRM731—borosilicate glass, certified from 80 to 680 K;

SRM736—copper, certified from 20 to 800 K; and

SRM738—stainless steel, certified from 293 to 980 K.

Accordingly, the shortage of reference materials usable at temperatures above 800 K is a problem one should not ignore.

Certified values of thermal expansion coefficients on reference materials should be determined using dilatometers based on absolute methods with a high resolution and accuracy. Optical interferometric dilatometers are ideal instruments for this purpose. Two types of dilatometers [1, 2], based on Fizeau and Michelson interferometers, were utilized for determining the certified values of the SRMs at NIST. Though capable of a high resolution and accuracy, these interferometers are not suitable for expansion measurements of solids at temperatures above 800 K. At high temperatures, problems associated with thermal stress, loss of mechanical strength, evaporation, etc., become severe, which lead to a variation of the do level of the interference fringe. In conventional interferometry, such as a Fizeau method, the dc level variation of the fringe increases the uncertainty in the determination of the fringe. Therefore, Okaji, one of the authors, has adopted an optical heterodyne interferometer for absolute measurements of thermal expansion coefficients of silicon in the temperature range 300 to 1300 K [3].

Compared to Fizeau interferometers, the optical heterodyne interferometer [4] is insensitive to the do level variation of the interference fringe. This insensitivity to the do level variation is achieved by the ac fringe detection method. Namely, the length change of the sample is measured by observing the shift in phase of the beat signal that is generated by two overlapping laser beams with a slight difference in frequency. In addition to the heterodyne technique, the interferometer adopted by Okaji employs a double-path optical system, which remarkably reduces the requirement for parallelism of the sample end faces before and during the measurement. Despite these effective techniques, there is considerable room for improvement in the dilatometer previously developed by Okaji for minimizing experimental uncertainties. The object of the present work is to develop an optical heterodyne interferometric dilatometer capable of

determining the linear thermal expansion coefficient, $\alpha(T)$, of a few suitable reference materials in the temperature range 300 to 1300 K. To measure $\alpha(T)$ with greater accuracy, refinements and improvements were made to most parts of the previous dilatometer, i.e., to the heating furnace, thermometer, optical arrangement, and optical devices. The performance of the present dilatometer was tested by comparing results of the linear thermal expansion coefficient of a single crystal of silicon with published data.

## 2. EXPERIMENTAL

### 2.1. Outline of Measurements

In the present study, values of $\alpha(T)$ were calculated by the following practical expression:

$$\alpha(T) = \Delta L/(L_{293}\, \Delta T) \tag{1}$$

where $\Delta T$ is a given temperature change from $T_1$ to $T_2$, $T$ is $(T_1+T_2)/2$, $L_{293}$ is the sample length at room temperature (293 K), and $\Delta L$ is the length change corresponding to $\Delta T$. Values of $\Delta L$, $\Delta T$, and $L_{293}$ were measured with a double-path optical heterodyne interferometer, a platinum-resistance thermometer, and a conventional micrometer, respectively. The measurements of $\Delta L$ and $\Delta T$ were made at predetermined stabilized temperatures in a stepwise heating cycle.

### 2.2. Measuring System

Figure 1 shows a schematic diagram of the measuring system. The system consists of a double-path optical heterodyne interferometer, an electric furnace with a carbon heater, a sample cell made of polycrystalline silicon, and a standard platinum-resistance thermometer (PRT). Details of the optical system of the interferometer are described in our previous papers [5, 6]. As shown in Fig. 1, laser beams from the interferometer pass into the furnace chamber through an optical window in the upper end of the chamber. The window was brought into thermal contact with a brass plate to minimize the temperature variation of the window. The temperature of the brass plate was stabilized to be 293 K using a thermoelectric transducer that was in thermal contact with the plate. The working space of the furnace is 38 mm in diameter and 100 mm in length.

Figure 2 shows the arrangement of the sample and a disc mirror used as the base plate in the sample cell. Both the sample and the base plate were cut from a silicon single-crystal rod grown by the floating zone

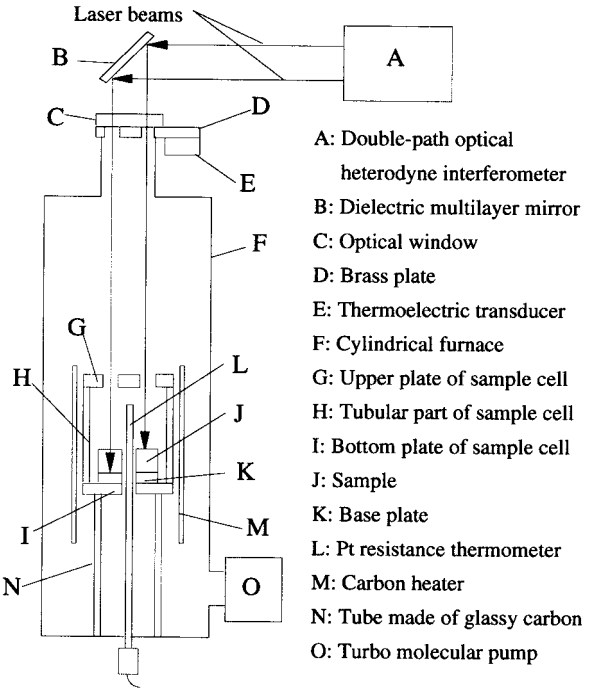


**Fig. 1.** Schematic diagram of the measuring system.

method. The sample was in the form of a perpendicular block whose size is $10 \times 7 \times 20$ mm. The $(7 \times 20)$ surfaces were polished to be flat to within one tenth of a wavelength of 632.8 nm and parallel within 5 arc s. The mirror face of the base plate was polished as was that of the sample. A hole having a diameter of 4 mm was bored down the symmetry axis through the optical flats of the sample and the base plate. The PRT used to measure the temperature of the sample was inserted into these holes. As shown in Fig. 2, the probe beams going along paths A and B are reflected normally at the sample and the base plate. A cube-corner prism in the interferometer returns the reflected beams to the sample cell. And so path A* corresponds to the second path of path A, and path B* to that of path B. The four paths are located at respective corners of a square of $10 \times 10$ mm on a plane perpendicular to the paths. This arrangement of the optical paths is an improvement on the previous interferometer developed by Okaji. This optical arrangement ensures that sufficient interference conditions are maintained even if the parallelism of the sample top face and the base plate is not preserved.

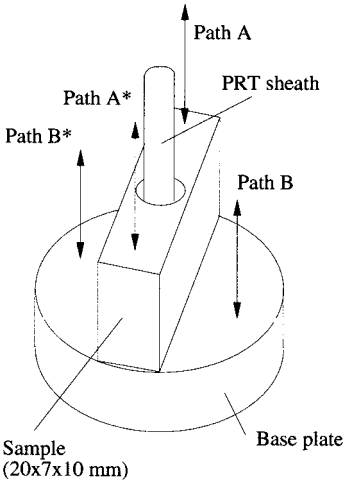


**Fig. 2.** Schematic diagram of the arrangement of the sample and base plate.

The PRT (Netsushin Model HIS-21-1000) [7] has a 3-$\Omega$ resistance at 273 K, and a current of 1 mA was chosen for all the measurements. The PRT satisfies ITS-90 requirements for the resistance ratio necessary for a Standard Temperature Measuring Instrument. The sensing element of the PRT is 30 mm long and 1.4 mm in diameter. The element consists of platinum wire having a diameter of 0.11 mm and a support made of alumina of 99.9 mass%. A fused-quartz tube 3 mm in diameter encases the element. The PRT sheath was inserted into the furnace along the central axis of the furnace.

## 2.3. Experimental Procedures

The sample was cleaned with hydrofluoric acid solution and then rinsed in distilled water, in anhydrous ethanol, and, finally, in acetone. The value of $L_{293}$ for the sample was determined to be 9.831 mm using a micrometer. The measurement of thermal expansion was carried out in the following manner. After the alignment of the sample and the probe beam was adjusted, the sample was heated to 1100 K to eliminate any tiny obstacles between the sample and the base plate. After that, the temperature of the sample was raised stepwise at intervals of about 50 K from 300 to 350 K and from 1250 to 1300 K, and at intervals of about 100 K from 350 to 1250 K. Temperature rates of change from one temperature step to the next were less than $1.8 \times 10^{-2}\,\mathrm{K \cdot s^{-1}}$. The temperature was kept at each of the steps for a time period longer than $1.8 \times 10^{3}\,\mathrm{s}$ to attain thermal equilibrium. The stepwise heating was controlled with a programmable control system whose

temperature-sensing element is a type C thermocouple located near the heater of the furnace. Differences between the temperature steps of the sample were measured with the PRT inserted into the hole of the sample and were used as values of $\Delta T$ in the calculation of $\alpha(T)$. In the experiment, the furnace was evacuated to $10^{-3}$ Pa with an oil-free turbomolecular pump.

## 3. RESULTS

### 3.1. Linear Thermal Expansion Coefficient of Si

The measurement of $\alpha(T)$ in the range 700 to 1100 K was repeated four times to evaluate the reproducibility of the results of the measurements. After each measurement run, the sample was removed from the sample cell and remounted, because the difference in position of the sample may cause a large uncertainty in the measured $\alpha(T)$. Figure 3 gives the present results of the repeated measurements on silicon, and the previous data measured by Okaji [3] and the CODATA recommended values [8, 9] for comparison. The solid curve shown in Fig. 3 represents a fourth-order polynomial function of temperature obtained from the least-squares fit to the present data. The fitting function for the range 700 to 1100 K is

$$\alpha(T)/(10^{-6}\,\mathrm{K}^{-1}) = -10.422 + 0.060977T - 9.7592\times10^{-5}T^2 + 7.0269\times10^{-8}T^3 - 1.8912\times10^{-11}T^4 \quad (2)$$

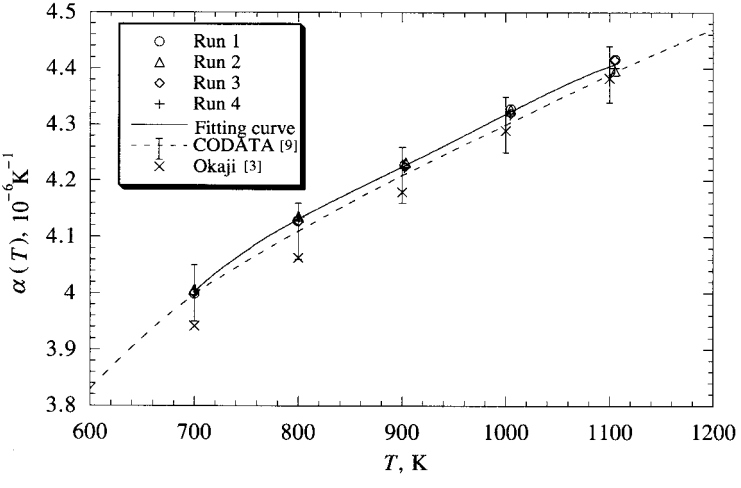


**Fig. 3.** Linear thermal expansion coefficients of silicon as a function of temperature.

The standard deviation of the experimental data from those calculated from the fitting function is estimated to be $5.4 \times 10^{-9}\ K^{-1}$. Our absence of data below 700 K and above 1100 K is explained below.

### 3.2. Zero Drift in Interferometric Signal

We decided the upper limit of the measurable temperature range on the basis of measurements of the zero drift in the interferometric signal. The zero drift means the apparent expansion (or contraction) arising from the imperfection of optical configurations of the interferometer and the sample. The zero drift was measured in the temperature range 300 to 1300 K by placing only the base plate in the sample cell. Figure 4 shows a typical result of the zero drift as a function of temperature. The absolute value of the zero drift increased with increasing temperatures, as shown in Fig. 4. Average magnitudes of the zero drift for three temperature ranges are listed in Table I. Each of the averages is calculated as the slope of linear functions of temperature obtained by a least-squares fitting procedure for the experimental value of the zero drift in the temperature range. It should be noted that the average zero drift for the temperature range 1200 to 1300 K is much greater than those for other two ranges. The drastic increase in the zero drift is due mainly to the occurrence of significant contamination of the sample. Silicon is prone to developments of its oxide layers at elevated temperatures, even under vacuum. In fact, the mirror face of the base plate tarnished after the temperature was raised above 1200 K

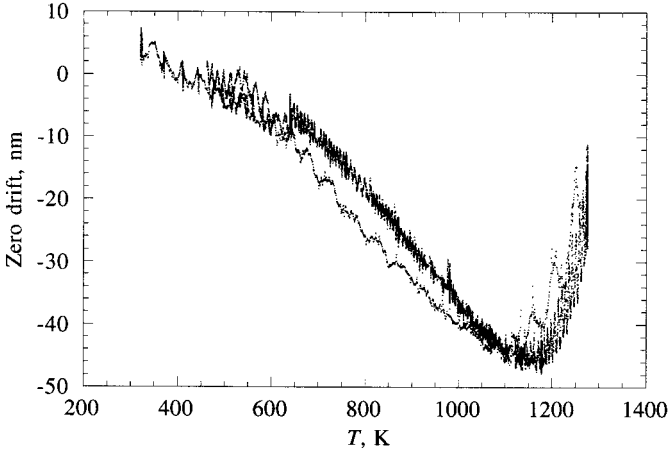


**Fig. 4.** The zero drift in the interference fringe against temperature.

**Table I.** Magnitude of the Zero Drift for Three Ranges of Temperature

| Temperature (K) | 330–600 | 600–1200 | 1200–1300 |
|---|---|---|---|
| Zero drift ($m \cdot K^{-1}$) | $-4.4 \times 10^{-11}$ | $-8.3 \times 10^{-11}$ | $+2.3 \times 10^{-10}$ |

several times. Accordingly, the $\alpha(T)$ on silicon above 1100 K was not determined in the present study.

### 3.3. Thermal Equilibrium Between the Sample and the PRT

The thermal equilibrium between the sample and the PRT has been taken into account for deciding the proper position of the sample in relation to the PRT. The thermal equilibrium between the sample and the PRT becomes poor if the sample is placed far away from the PRT. To measure the sample temperature with sufficient accuracy, the sample should be located within an allowable range from the position of the PRT element. The allowable range in the present study was experimentally determined in the following manner. The center of the PRT element was fixed at a specific point ($H_0$), where the temperature was the highest of the points along the central axis of the furnace. On the other hand, the position of the sample could be shifted along the central axis by replacing the bottom plate of the sample cell with one with a different thickness. Figure 5 shows the comparison of three data sets of $\alpha(T)$ measured when the center of the

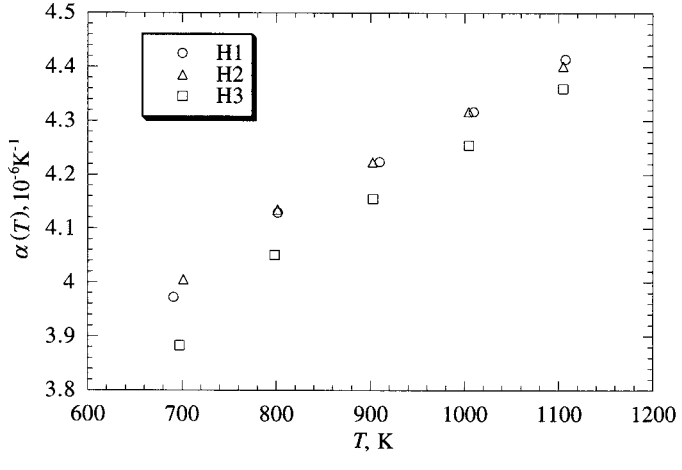


**Fig. 5.** Comparison of three data sets of $\alpha(T)$ measured when the sample was located at three points (H1, H2, and H3).

sample was located at three points, H1, H2, and H3. Point H1 was positioned 2.5 mm below, H2 was 3.5 mm above, and H3 was 8.5 mm above point $H_0$. As shown in Fig. 5, the data measured for H1 and H2 are in good agreement with each other but the data for H3 are systematically lower than other values. These findings suggest that points H1 and H2 are within the allowable range. Accordingly, the values of $\alpha(T)$ shown in Fig. 3 were measured when the center of the sample was located at point H1.

The lower limit of the measurable temperature range was also imposed by the need to have a sufficient thermal equilibrium between the sample and the PRT. At temperatures lower than 700 K, good thermal contact between the sample and the PRT was difficult to achieve even if the sample was placed at the point H1. This can be explained in terms of the decrease in thermal conductivity with decreasing temperatures. Considering this fact, the $\alpha(T)$ of silicon at temperatures below 700 K was not determined in the present study.

## 4. DISCUSSION

### 4.1. Estimate of Uncertainty

The combined standard uncertainty ($\Delta\alpha_C$) in the measured value of $\alpha(T)$ at 900 K is estimated to represent the average magnitude of the uncertainties for the temperature range 700 to 1100 K. In this work, it is assumed that magnitudes of major uncertainties are obtained by a Type A evaluation. Therefore, the value of $\Delta\alpha_C$ is calculated using the following equation:

$$\Delta\alpha_C = \sqrt{(\Delta\alpha_L)^2 + (\Delta\alpha_T)^2 + (\Delta\alpha_{L293})^2}$$

$$\Delta\alpha_L = \frac{\alpha\delta(\Delta L)}{\Delta L}, \qquad \Delta\alpha_T = \frac{\alpha\delta(\Delta T)}{\Delta T}, \qquad \text{and} \qquad \Delta\alpha_{L293} = \frac{\alpha\delta L_{293}}{L_{293}} \tag{3}$$

where $\delta(\Delta L)$, $\delta(\Delta T)$, and $\delta L_{293}$ are the uncertainties of $\Delta L$, $\Delta T$, and $L_{293}$, respectively. Sources and magnitudes of uncertainty in $\alpha(T)$ at 900 K are listed in Table II. The magnitudes of uncertainties are estimated under the condition that $L_{293}$ is 10 mm and $\Delta T$ is 100 K. In addition, the value of $\alpha(T)$ at 900 K calculated from Eq. (2) is used in the estimation of the uncertainty.

The dominant source of $\delta(\Delta L)$ was the zero drift in the interferometric signal. The magnitude of $\delta(\Delta L)$ at 900 K is shown as $8.3 \times 10^{-11}$ m·K$^{-1}$ in Table I, and thus, the magnitude of $\Delta\alpha_L$ caused by the zero drift is estimated to be $8.3 \times 10^{-9}$ K$^{-1}$. The magnitude of $\delta(\Delta L)$ for the interferometer linearity was measured as the zero drift when the temperature of the base plate is

**Table II.** Sources and Magnitudes of Uncertainty in $\alpha(T)$ at 900 K

| Temperature, $T$<br>$\alpha$[a] | 900 K<br>$4.22 \times 10^{-6}$ ($K^{-1}$) | |
|---|---|---|
| Uncertainty sources | Magnitude of Uncertainties[b] | |
| | $\delta(\Delta L)$ | $\Delta\alpha_L$($K^{-1}$) |
| Zero drift | 8.3 nm | $8.3 \times 10^{-9}$ |
| Interferometer linearity | 0.57 nm | $5.7 \times 10^{-10}$ |
| Laser frequency stability | 0.041 nm | $4.1 \times 10^{-11}$ |
| | $\delta(\Delta T)$ | $\Delta\alpha_T$ ($K^{-1}$) |
| Temperature nonuniformity within sample | 0.15 K | $6.3 \times 10^{-9}$ |
| Thermometer calibration | $1.2 \times 10^{-2}$ K | $5.1 \times 10^{-10}$ |
| Stability of the PRT | $7 \times 10^{-3}$ K | $3.0 \times 10^{-10}$ |
| | $\delta L_{293}$ | $\Delta\alpha_{L293}$($K^{-1}$) |
| Determination of $L_{293}$ | $5 \times 10^{-6}$ m | $2.1 \times 10^{-9}$ |
| Combined standard uncertainty, $\Delta\alpha_c$($K^{-1}$) | | $1.1 \times 10^{-8}$ |
| Relative value of $\Delta\alpha_c$, $(\Delta\alpha_c/\alpha) \times 100$ | | 0.26% |

[a] Calculated from Eq. (2).
[b] Estimated under the condition that $L_{293}$ is 10 mm and $\Delta T$ is 100 K.

maintained at room temperature for $9 \times 10^4$ s. The magnitude of $\delta(\Delta L)$ for the laser frequency stability is provided from the manufacturer of the laser (Melles-Griot Model 05STP901). The uncertainty of $\Delta\alpha_T$ arises predominantly from the inhomogeneous temperature distribution within the sample. The temperature difference within the sample at 900 K is less than $1.5 \times 10^{-1}$ K. Thus the magnitude of $\Delta\alpha_T$ due to the temperature distribution is calculated to be less than $6.3 \times 10^{-9}$ $K^{-1}$. The uncertainty associated with the stability of the PRT was estimated from the measurement of the drift in the resistance of the PRT at the triple point of water. The resistance is expected to show a drift of $7 \times 10^{-3}$ K after the PRT is exposed to 1100 K for 10 h [7]. Using the magnitude of the drift, the uncertainty associated with the PRT stability is calculated to be $3 \times 10^{-10}$ $K^{-1}$. The temperature is determined by substituting the measured resistance of the PRT into the temperature characteristic function specified by a practical correction method. The function was practically corrected by the measurement at the solidification point of indium (429.7 K). The uncertainty in temperature due to the thermometer calibration was expected to be less

than $1.2 \times 10^{-2}$ K and thus its contribution is estimated to be $5.1 \times 10^{-10}$ $K^{-1}$. Details of the practical correction using only one fixed point are described in Ref. 7. The magnitude of $\Delta\alpha_{L293}$ was estimated to be $2.1 \times 10^{-9}$ $K^{-1}$ from the $\delta(\Delta L_{293})$ of $5 \times 10^{-6}$ m, which is the standard deviation of the measured $L_{293}$ from the average of eight determinations. With the values of these uncertainties, the magnitude of $\Delta\alpha_C$ at 900 K is calculated to be $1.1 \times 10^{-8}$ $K^{-1}$ from Eq. (3).

### 4.2. Comparison with Published Values

In Fig. 3 the cross denotes the data measured by Okaji using the previous version of the optical heterodyne interferometric dilatometer [3]. The present data are higher than the previous data, and the discrepancy between them increased as the temperature decreases. The discrepancy suggests that the previous data have some uncertainties due to systematic effects that can be minimized in the present study. Compared to the previous dilatometer, the present one has some advantages of minimizing the uncertainties associated with the following factors: (1) thermal equilibrium between the sample and the thermometer, (2) long-term stability of the thermometer, and (3) the so-called mixing problem [5] in polarization interferometry. In the previous study, the sample was rapidly heated with a radiant image furnace. High-speed heating with a radiant image furnace may lead to a large temperature difference between the sample and the thermometer or a serious nonuniformity in temperature within the sample. In contrast, the sample used in the present study was gradually heated with an electric furnace to promote thermal equilibrium between the sample and the PRT. The relatively large discrepancy at lower temperatures may be responsible for the insufficient thermal equilibrium of the sample in the previous study, because the thermal equilibrium between the sample and the thermometer became poorer at lower temperatures.

In the previous dilatometer, an R-type thermocouple was used to measure the sample temperature. Compared to the PRT used in the present work, the R-type thermocouple is sufficiently sensitive but lacks long-term stability. The uncertainty associated with the third factor results from the use of a Zeeman laser as the coherent light source for the heterodyne interferometry in the previous dilatometer. Mixing the two optical components that a practical Zeeman laser emits results in a systematic uncertainty in the expansion measurement [5]. In the present interferometer the probe and reference laser beams were generated using the combination of a He–Ne laser unit and a pair of acoustooptical modulators to avoid the mixing effect [5]. From these merits of the present dilatometer, we can conclude that the performance of the present dilatometer is more effective than that of the previous one. In fact, the standard deviation of data points

($5.4 \times 10^{-9}\ K^{-1}$) from the best least-squares fit for the present study is lower than that for the previous study ($2.1 \times 10^{-8}\ K^{-1}$).

The dashed curve shown in Fig. 3 corresponds to the recommended values by CODATA [8, 9]. Error bars of the dashed line represent maximum probable errors of the recommended values and are estimated to be $5 \times 10^{-8}\ K^{-1}$. Differences between the present data and the recommended values are within the maximum probable errors. The recommended values are given by a fitting procedure for five sets of experimental data, including the previous data measured by Okaji, into the Einstein function for heat capacity plus an error term. Because of the shortage of high-temperature data, only the previous data by Okaji were used for the evaluation of the recommended values at temperatures above 850 K. Therefore, the recommended values at temperatures below 850 K are more reliable than those at temperatures above 850 K. In contrast to the previous data by Okaji, the present data are in good agreement with the recommended values even at lower temperatures, which validates the performance of the present dilatometer.

## 5. CONCLUSIONS

An optical heterodyne interferometric dilatometer has been developed and tested. Linear thermal expansion coefficients of silicon were measured in the temperature range 700 to 1100 K. The standard deviation of the measured values from those calculated from the best least-squares fit is $5.4 \times 10^{-9}\ K^{-1}$. The comparison of the present data and published data shows that the present dilatometer is an ideal tool for determining linear thermal expansion coefficients of reference materials in the temperature range 700 to 1100 K. The present data are in good agreement with the CODATA recommended values. Expanding the measurable temperature range of the dilatometer is a subject for future study.

## REFERENCES

1. T. A. Hahn, *J. Appl. Phys.* **41**:5096 (1970).
2. A. P. Miiller and A. Cezairliyan, *Int. J. Thermophys.* **6**:695 (1985).
3. M. Okaji, *Int. J. Thermophys.* **9**:1101 (1988).
4. M. Tanaka, T. Yamagami, and K. Nakayama, *IEEE Trans. Instrum. Meas.* **38**:552 (1989).
5. M. Okaji and N. Yamada, *High Temp. High Press.* **29**:89 (1997).
6. H. Watanabe, N. Yamada, and M. Okaji, *Int. J. Thermophys.* **22**:1185 (2001).
7. M. Arai, in *Proc. 6th Int. Symp. on Temp. Therm. Measur. Industry Sci.*, Torino, Italy (1996), pp. 135– 139.
8. C. A. Swenson, *J. Phys. Chem. Ref. Data* **12**:179 (1983).
9. G. K. White and M. L. Minges, *Int. J. Thermophys.* **18**:1269 (1997).